Cardiovasc Eng
DOI 10.1007/s10558-007-9047-3

ORIGINAL PAPER

Sensitivity Analysis and Model Assessment: Mathematical Models for Arterial Blood Flow and Blood Pressure

Laura M. Ellwein · Hien T. Tran · Cheryl Zapata · Vera Novak · Mette S. Olufsen

Abstract The complexity of mathematical models describing the cardiovascular system has grown in recent years to more accurately account for physiological dynamics. To aid in model validation and design, classical deterministic sensitivity analysis is performed on the cardiovascular model first presented by Olufsen, Tran, Ottesen, Ellwein, Lipsitz and Novak (J Appl Physiol 99(4):1523–1537, 2005). This model uses 11 differential state equations with 52 parameters to predict arterial blood flow and blood pressure. The relative sensitivity solutions of the model state equations with respect to each of the parameters is calculated and a sensitivity ranking is created for each parameter. Parameters are separated into two groups: sensitive and insensitive parameters. Small changes in sensitive parameters have a large effect on the model solution while changes in insensitive parameters have a negligible effect. This analysis was successfully used to reduce the effective parameter space by more than half and the computation time by two thirds. Additionally, a simpler model was designed that retained the necessary features of the original model but with two-thirds of the state equations and half of the model parameters.

Keywords Cardiovascular modeling · Sensitivity analysis · Model reduction · Parameter estimation

L. M. Ellwein · H. T. Tran · C. Zapata · V. Novak · M. S. Olufsen (✉)
Department of Mathematics, North Carolina State University, Raleigh, NC 27695, USA
e-mail: msolufse@math.ncsu.edu

Introduction

During the last decades a large number of lumped parameter differential equations models have been developed to study dynamics and control of the cardiovascular system, see e.g., Kappel and Peer (1993), Olufsen et al. (2005), Olufsen et al. (2006), Ottesen (1997a, b), Rideout (1991), and Ursino (1998). Typically, these models predict blood pressure and flow in and between compartments representing various parts of the cardiovascular system using electrical circuits with capacitors and resistors. In the recent years the complexity of these models have increased to more accurately account for the underlying physiological dynamics. For example, complex nonlinear models have been developed to describe the pulsatile pumping of the heart, e.g., Danielsen and Ottesen (2001), Ottesen and Danielsen (2003), and Olufsen et al. (2005), and the blood flow and blood pressure regulation, Olufsen et al. (2004), Olufsen et al. (2005), Heldt et al. (2002), and Ursino (1998). These complex nonlinear models often include a large number of parameters. While physiological knowledge can be used to determine nominal values for some of these parameters, several parameters can only be estimated based on observations from animal studies, and some parameters cannot be determined at all. Simulations using nominal parameter values may provide insight into the overall model dynamics and the behavior for a given group of subjects, but since physiological properties are known to vary significantly between subjects, such simulations cannot provide patient specific information.

One way to obtain patient specific information is to solve the inverse problem: identifying model parameters given measured observations and the mathematical model. This can be done using non-linear optimization techniques for example, as described by Kelley (1999). However,

these techniques have mostly been used for simpler problems with a small number of paramters or for problems where most of the internal states can be determined. For complex nonlinear problems with many states and parameters, where only a limited number of states can be observed, these techniques give rise to non-unique solutions and they often result in numerical problems since the differential equations may be stiff, contain delays, or be ill-posed. In this study, we plan to use sensitivity analysis as described by Eslami (1994) and Frank (1978), to separate a large set of parameters into two groups: sensitive parameters (parameters for which a small change in the parameter value gives rise to a large change in an observed state) and insensitive parameters (parameters for which a small change in their values does not significantly affect the dynamics of one of the observed states). The goal of our study is to show that it is possibly to only "identify" sensitive parameters while the "insensitive parameters" can be kept at their nominal values. This information can also be used to obtain a better understanding of the model behavior and to provide information for model reduction and simplification.

In this study, we analyzed a cardiovascular model with 11 compartments developed to predict the effect of postural change from sitting to standing using measurements of finger blood pressure and cerebral blood flow velocity. This model predicts arterial and venous blood pressures as well as the volume of the heart using a system of 11 coupled differential equations that are functions of 52 model parameters. Unique identification of all 52 parameters is not possible, and even obtaining approximate estimations for these parameters is time consuming. Furthermore, the computed outcome states at locations where data are measured (i.e., finger blood pressure and cerebral blood flow velocity) may not be sensitive to all 52 parameters.

Sensitivity analysis methodologies can be formulated either using a stochastic or a deterministic approach. In this study we only discuss deterministic methodologies. These can be divided into two groups: studies that examine local sensitivities, obtained by studying the effect of small perturbations of the model parameters, and studies that examine global sensitivities, obtained by examining the model dynamics of a large parameter space. Sensitivity analysis has been used over the last several years to analyze models in other sciences, but to our knowledge this type of analysis has not been used extensively for the analysis of physiological models. Previous studies include work by Ebert (1985), who performed a local sensitivity analysis using analytic derivatives to understand what parameters that had the greatest impact on sea urchin growth, while Carmichael et al. (1997) compared three local sensitivity methods, all using automatic differentiation, to analyze the impact of parameter perturbations on atmospheric ozone. Rabitz et al. (1983) discuss both local and global methods in the context of a system of ordinary differential equations (ODEs) that describe chemical kinetics.

For all of the above studies the goal was to derive sensitivity information to better understand the model dynamics, but was not used for further model development. We will focus on using sensitivities for model assessment and development. We adopt a similar procedure as Banks and Bortz (2005) and Bortz and Nelson (2004), but take the analysis a step further using sensitivity ranking results to shorten the parameter identification computational time and simplify the model.

In the following, we provide a description of the mathematical model and experimental setup. Subsequently, sensitivity analysis and special considerations important for analysis of the blood flow model will be described. Finally, we describe sensitivity results and discuss how these can be used to design the simplest possible model that can predict dynamics observed in experimental data.

Methods

The 11 compartment model to be analyzed (see Fig. 1a) was originally developed to understand dynamics of cerebral blood flow velocity and finger blood pressure during postural change from sitting to standing, Olufsen et al. (2004, 2005). To understand this process, the model included three states: (i) sitting, also referred to as "steady-state", where limited regulation occurs; (ii) transition from sitting to standing including the initial gravitational response leading to pooling of blood in the legs; and (iii) standing, where short-term regulatory mechanisms are activated to bring blood pressure and blood flow from decreased values back to steady-state.

Current physiological knowledge suggests that the majority of these control mechanisms occur in systemic circulation. Furthermore, data to be analyzed were all measured in the systemic circulation. Thus the model to be studied only comprised the systemic circulation. This simplification of the model design was essential, since it allowed us to only represent one side of the heart, namely the left atrium and the left ventricle. To dynamically describe the blood flow and blood pressure and their control during postural change, it is important to describe flow of blood, including how vessel tone, vessel diameters, heart rate, and cardiac contractility (included in the heart model) are modulated during postural change. To understand the system dynamics the model included elements that can represent these quantities. To understand the controlled response, it was necessary to include a model that described how this response was evoked. Physiologically, standing up leads to pooling of blood in the legs. Thus the

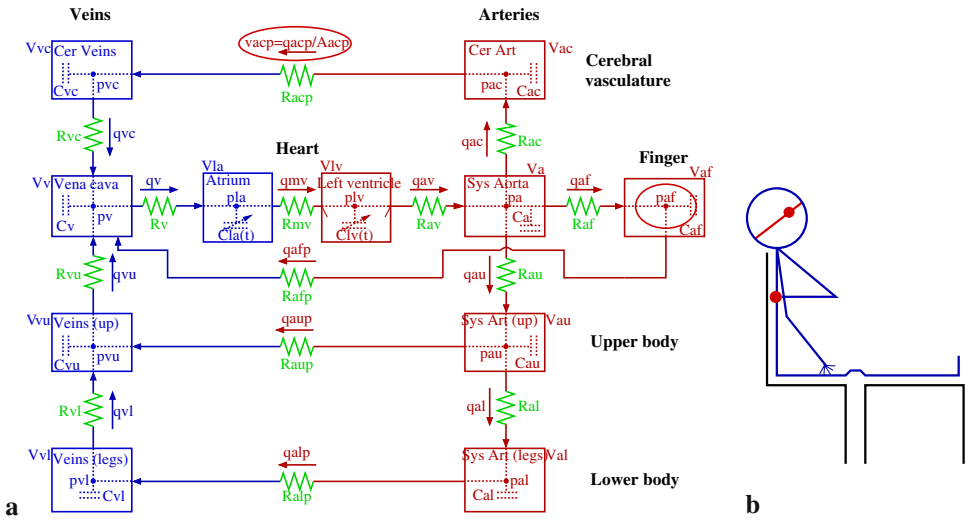

Fig. 1 (**a**) The 11 compartment model electrical circuit analog of the systemic circulation, including arteries (a) and veins (v) in the brain (cerebral vasculature, c), the upper body (u), the legs (lower body, l), the finger (f), the left atrium (la), and the left ventricle (lv). Flow through the model is defined by q (cm^3/s). Pressures and volumes related to each compartment are marked by p (mmHg) and V (cm^3), respectively. Resistors are denoted by R (mmHg s/cm^3) and capacitors by C (cm^3/mmHg). Resistors R_{acp}, R_{aup}, R_{alp}, and R_{afp} represent the peripheral vascular bed. The mitral and aortic valves are marked by small lines inside the compartment representing the left ventricle. Blood pressure p_{af} (mmHg) was measured in the finger and blood flow velocity $v_{\text{acp}} = q_{\text{acp}}/A_{\text{acp}}$ (cm/s) was measured in the middle cerebral artery (marked with circles on the figure), where A_{acp} (cm^2) is vessel cross-sectional area. (**b**) The experimental setup, with blood pressure and blood flow velocity measurement locations marked with filled circles

model included compartments that comprised arteries and veins in the upper body and in the legs. To predict responses observed in data the model included one compartment representing the finger, and two compartments representing the flow to the brain. Finally, to generate the pulse-wave pumped through the circulation, the model included compartments representing the left atrium and the left ventricle. The resulting model arising from these considerations is shown in Fig. 1a. To illustrate the ideas proposed in this study, we focus on analyzing the steady-state (sitting) portion of the model.

Model Equations

Similar to previous studies, Olufsen et al. (2004, 2005), the model is depicted using an electrical circuit analog in which pressure $p(t)$ (mmHg) compares to voltage and volumetric flow rate $q(t)$ (cm^3/s) is analogous to current. Compliance C (cm^3/mmHg) plays the role of capacitance and is a measure of vessel tone (stiffness), and resistance R (mmHg s/cm^3) is the same in both environments. Below we describe the derivation of the model. A complete list of all equations can be found in the Appendix, a list of state variables can be found in Table 1, and the model parameters are listed in Table 4. For each of the arterial and venous compartments (i.e., neither of the heart compartments), pressure $p_i(t)$ is determined by differentiating the volume equation $V_i(t) - V_{\text{unstr},i} = C_i p_i(t)$, where $V_i(t)$ (cm^3) is the time-dependent volume, $V_{\text{unstr},i}$ (cm^3) (constant) is the unstressed volume, and C_i is the compliance (constant). Differentiating this equation gives

$$C_i \frac{dp_i}{dt} = \frac{dV_i}{dt} = q_{\text{in}} - q_{\text{out}}, \text{ where}$$
$$q_{\text{in}} = \frac{p_{i-1} - p_i}{R_{\text{in}}}, \quad q_{\text{out}} = \frac{p_i - p_{i+1}}{R_{\text{out}}}. \tag{1}$$

In the above equation, the state variables are pressures p_i and the model parameters to be identified are R_i and C_i. The subscript i designates the particular compartment, thus $i-1$ and $i+1$ refer to upstream and downstream

Table 1 Description of the state variables (a list of the model parameters can be found in Table 4), also see Fig. 1 for the locations of the states

State variable	Description
p_{a}	Pressure in the aorta
p_{af}	Pressure in the finger arteries
p_{au}	Pressure in the upper body arteries
p_{al}	Pressure in the lower body arteries
p_{vl}	Pressure in the lower body veins
p_{vu}	Pressure in the upper body veins
p_{v}	Pressure in the vena cava
p_{vc}	Pressure in the cerebral veins
p_{ac}	Pressure in the cerebral arteries
V_{la}	Volume in the left atrium
V_{lv}	Volume in the left ventricle

compartments, respectively. The 11 compartment model has nine of these equations, one for each of the arterial and venous pressures. For example, the change in arterial finger pressure p_{af}, becomes

$$\frac{dp_{\text{af}}}{dt} = \frac{1}{C_{\text{af}}}\left(\frac{p_{\text{a}} - p_{\text{af}}}{R_{\text{af}}} - \frac{p_{\text{af}} - p_{\text{v}}}{R_{\text{afp}}}\right), \tag{2}$$

where p_{af}, p_{a}, and p_{v} represent model states and C_{af}, R_{af}, and R_{afp} are the model parameters.

To close the system of equations, two additional equations are required. These can be obtained by ensuring that volume is conserved in the left atrium (la) and ventricle (lv), i.e., we assume that

$$\frac{dV_j}{dt} = q_{\text{in}} - q_{\text{out}}, \quad j = \text{la, lv}. \tag{3}$$

In these equations the flows are determined using Ohm's law for hemodynamics. The latter equations are described in terms of volume, but pressures are needed to determine the flow. Pressures in the vessel compartments are found from solutions to (1); however, additional equations are required to determine pressures in the left atrium and ventricle. For the 11 compartment model, these pressures are explicitly stated to account for the pumping action of the heart.

Several such models exist in the literature. We use the model from previous work, proposed by Ottesen and Danielsen (2003). This model computes a time-varying pressure in the left atrium and ventricle as

$$p_j = a_j(V_j - b_j)^2 + (c_j V_j - d_j)\, f_j(t, H), \quad j = \text{la, lv}. \tag{4}$$

Again, this equation is valid for both the left atrium ($j = \text{la}$) and the left ventricle ($j = \text{lv}$). In this equation V_j is the volume of the left atrium or the left ventricle, respectively. These volumes are state variables calculated using (3). Parameters for this equation include a_j,b_j,c_j, and d_j, while f_j is an activation function varying between 0 and 1. The parameter a_j (mmHg/cm^3) represents the atrial/ventricular elastance during relaxation and b_j (cm^3) represents the atrial/ventricular volume at zero diastolic pressure. The parameters c_j (mmHg/cm^3) and d_j (mmHg) relate to the volume dependent (contractility) and volume independent components of the developed pressure. The activation function $f_j(t,H)$, a function of time t (s) and heart rate H (beats/s) is described by a polynomial of the form

$$f_j = \begin{cases} \tilde{p}_j(H)\dfrac{\tilde{t}^{n_j}(\beta_j(H) - \tilde{t})^{m_j}}{n_j^{n_j} m_j^{m_j}[(\beta_j(H))/(m_j + n_j)]^{m_j+n_j}} & 0 \le \tilde{t} \le \beta_j(H), \quad j = \text{la, lv} \\ 0 & \beta_j(H) < \tilde{t} < T. \end{cases} \tag{5}$$

Here $\tilde{t} = \text{mod}(t, T)$ (s), T being the period of a single heart beat, $\tilde{p}_j(H)$ is the peak pressure, and $\beta_j(H)$ is a sigmoidal function of the heart rate H (beats/s). This function resets with every heart beat and it is smooth. The pumping model discussed above does not give rise to additional state variables, yet it does have a significant number of parameters. The left atrium and ventricle functions each contain 14 parameters: four parameters are included in (4) and the activation function f_j contains 10 parameters.

Equation (3) does not account for the change in flow due to the presence of the valves controlling flow into (the mitral valve) and out of (the aortic valve) the left ventricle. These valves are important to ensure that blood flows in the correct direction. At the start of the cardiac cycle, the aortic valve is closed while the mitral valve is open, allowing blood to enter the ventricle at a low pressure. When the ventricular pressure exceeds that of the atrium, the mitral valve is closed. After closure of the mitral valve, ventricular contraction increases ventricular pressure until it exceeds aortic pressure, causing the aortic valve to open and blood to be ejected into the aorta. The aortic valve closes when the cycle is completed. Note that for healthy subjects, the population from which our data comes, at no time are both valves open. This action of the valves introduces discrete behavior into the model, since the flow out of the left ventricle is either 0 (when the valve is closed) or, e.g., $q_{\text{av}} = (p_{\text{lv}} - p_{\text{a}})/R_{\text{av}}$. One way to account for this "switch" is by introduction of discrete events triggered by changes in pressure. However, this approach would make it difficult to use differential sensitivity analysis to determine sensitivity of model parameters. Another approach, also used in previous work, e.g., Olufsen et al. (2004, 2005), is to model the succession of opening and closing of the valves using varying resistances. This can be done using a small baseline resistance to define the "open" valve and a resistance that is several orders of magnitude larger to define the "closed" valve. For example, the aortic valve resistance can be defined by

$$R_{\text{av}} = \min\left[R_{\text{av,open}} + \exp\left(-2(p_{\text{lv}} - p_{\text{a}})\right), 20\right]. \tag{6}$$

In this equation, the transition from open to closed is gradual. An exponential function is used to describe the amount of "openness" as a function of the pressure gradient. Values in the exponent are chosen to ensure that the valve closes efficiently and that the effective flow is zero while the valve is closed.

In summary, the cardiovascular system is described by system of 11 coupled nonlinear first order differential equations predicting changes in pressure and volume as functions of 52 model parameters. This system comprises nine equations of the form given in (1) predicting arterial and venous pressures and two equations of the form given in (3) predicting atrial and ventricular volumes. Coupled with these differential equations are five algebraic equations, two equations predicting pressure in each of the ventricles (4) and three equations describing the resistance of the mitral and aortic valves, and also a venous valve (6). The latter is included to prevent reverse flow in legs. For completeness, these equations are given in their entirety in the Appendix. The 52 model parameters include 14 resistors, 9 capacitors, 28 heart parameters, and a scaling factor relating cerebral blood flow (predicted by the model) to cerebral blood flow velocity (measured experimentally). This system of equations can be written as

$$\frac{dX}{dt} = F(X, t, \mu), \tag{7}$$

where $X(X,t,\mu) = [p_a \ \ldots \ p_{vc}, V_{lv}, V_{la}]$ denotes the 11 state variables and $\mu = [\mu_1 \ \ldots \ \mu_{52}]$ denotes the 52 parameters to be identified. In the following analysis, we use this notation to discuss the dynamics of the model.

Model Parameters

Nominal parameter values for all resistors and capacitors for a healthy young subject were determined using theoretical considerations for blood pressure, flow, and volume distribution between organs. Compliances can be estimated using the volume pressure relation, which requires estimation of both total and unstressed blood volumes. Total blood volumes cannot easily be measured but experimental studies suggest to estimate volumes using Nadler's formula Nadler et al. (1962) which for the healthy subject analyzed in this study gives $V_T = 4673$ ml. Unstressed volumes are difficult to estimate. To our knowledge, only one study Beneken and DeWit (1967) has attempted to estimate V_{unstr}. In addition to volume, it is necessary to use estimates of blood pressure to estimate compliance for each compartment. Standard values for blood pressure are more easily obtained from the literature; however, for consistency we used Beneken and DeWit (1967) values for both blood pressure and blood volumes. To adjust pressures for the subject in question, we assumed that the nominal estimate for the finger pressure matched the mean arterial pressure obtained from Portapress measurements. Using these values, initial compliances for each compartment were calculated as $(V_{T,i}) \cdot (\%\,\text{stressed})/\bar{p}_i$, with volume $V_{T,i}$ being the total volume for compartment i. Note that since the model only contains the systemic circulation, the sum of volumes for each of the nine arterial and venous compartments equals the total volume of the cardiovascular system V_T minus the volume of the pulmonary system. Resistances are calculated using estimates of cardiac output and information on the distribution of blood flow to the different regions in the body. Cardiac output was estimated from the total blood volume using the assumption that the entire blood volume circulates within one minute, Boron and Boulpaep (2003). Several studies provide information on blood flow to the different regions of the body, e.g., Beneken and DeWit (1967), Bischoff and Brown (1966), and Middleman (1972). For consistency with estimates on unstressed volumes we used values from Beneken and DeWit (1967), scaled using the subject's blood volume to estimate average blood flow rates $\bar{q}_i$ to each compartment. Initial resistances were then calculated $(\bar{p}_{in,i} - \bar{p}_{out,i})/\bar{q}_i$ for each branch. All values used in calculations for C and R are given in Tables 2 and 3.

Parameter values for the left ventricle were taken from work by Ottesen and Danielsen (2003). These parameters were mostly estimated based on data from a dog heart ventricle. To estimate parameters for the left atrium we scaled the ventricle parameters to account for the difference in magnitude between atrial and ventricular systolic pressure. All of these parameter values are given in Table 4. Finally, the scaling parameter A_{acp} (cm^2), a lumped cerebral vasculature cross-sectional area, was estimated by calculating the approximate cross-sectional area of the middle cerebral artery in which velocity is measured, i.e., $q_{acp} = v_{acp}A_{acp}$.

Using these nominal parameter values including 14 resistors, 9 capacitors, and 28 parameters used in the pumping functions for the left atrium and ventricle (see Table 4) we solved the model equations and compared computed solutions with measurements of finger blood pressure and cerebral blood flow velocity for a healthy young subject, see Fig. 2. It should be noted that while our nominal parameter values provided fairly good estimates for blood pressure the estimates for cerebral blood flow velocity are too low (though they are within a physiological range). This is partly due to our assumption that brain compartments are assumed to represent the total flow to the brain, while data are measured in a single artery (the middle cerebral artery) and partly due to the estimates for unstressed volumes, which have a high level of uncertainty.

Experimental Data

This study uses data from one healthy young subject who had no known systemic disease, no history of head or brain injury, no history of more than one episode of syncope, and

Table 2 Compliance estimates giving the ratio of the effective volume to the pressure. Pressures were estimated from patient data. All other data was estimated from Beneken and DeWit (1967) and scaled based on patient anthropomorphic data. See Fig. 1 for location of the components

Compartment	Pressure (mmHg)	Total volume (ml)	Percent stressed	Effective volume (ml)	Compliance (ml/mmHg)
Aorta (a)	73	92.7	35	32.4	0.444
Upper body arteries (au)	70	384.8	30	115.4	1.649
Lower body arteries (al)	68	84.8	16	13.6	0.200
Cerebral arteries (ac)	70	99.0	25	24.7	0.354
Finger arteries (af)	72.8	33.6	25	8.4	0.115
Vena cava (v)	4	599.1	8	47.9	11.982
Upper body veins (vu)	6	1961.5	8	156.9	26.154
Lower body veins (vl)	8	333.5	8	26.7	3.335
Cerebral veins (vc)	10	402.0	20	80.4	8.040
Ventricle systolic (lv)	73.5	–	–	–	–
Ventricle diastolic (lv)	2	–	–	–	–
Atrium pressure (la)	3	–	–	–	–

Table 3 Initial resistances and flowrates for each pathway. Flow percentages are from Beneken and DeWit (1967), and scaled based on estimated patient blood volume. Resistances are calculated using Poiseuille's law, $R_i = (\bar{p}_{\text{in}} - \bar{p}_{\text{out}}/\bar{q}_i)$. See Fig. 1 for location of components

Pathway	Segment	Percent of cardiac output	Flowrate (ml/s)	Resistance, PRU (mmHg s/ml)
q_{av}	Cardiac output	100	77.883	0.006
q_{au}	Upper body	64	62.307	0.048
q_{aup}	Upper body	64	49.845	1.284
q_{al}	Lower body	8	6.231	0.321
q_{alp}	Lower body	8	6.231	9.630
q_{ac}	Cerebral (Brain)	20	15.577	0.193
q_{acp}	Cerebral (Brain)	20	15.577	3.852
q_{af}	Finger (Arm)	8	6.231	0.032
q_{afp}	Finger (Arm)	8	6.231	11.042
q_{vl}	Lower body	8	6.231	0.321
q_{vu}	Upper body	64	62.307	0.032
q_{vc}	Cerebral (Brain)	20	15.577	0.385
q_{v}	Cardiac output	100	77.883	0.013

took no cardiovascular medications, see Fig. 2. Measurements analyzed in this study include beat-to-beat arterial pressure obtained from a cuff placed on the finger using a Portapress-2 device (FMS, Inc.) and beat-to-beat middle cerebral blood flow velocity measurements from the index finger obtained using a Transcranial Doppler (TCD) system (MultiDop X4, Neuroscan, Inc.). Data analyzed in this manuscript was recorded continuously during a 5 min interval while the subject sat on a chair with their legs elevated at 90 degrees to reduce venous pooling. After the subject was asked to stand, recordings were continued for an additional 5 min period, see Fig. 1b. All analog signals was recorded at 500 Hz using Labview NIDAQ (National Instruments Data Acquisition System 64 Channel/100 Ks/s, Labview 6i, Austin, TX) on a Pentium Xeon 2 GHz dual processor computer and stored for offline processing. Prior to analysis, data were down-sampled to 50 Hz. All data was visually inspected for accuracy of R-wave detection, artifacts, and occasional extra systoles that were removed using a linear interpolation algorithm. Data was collected in the Syncope and Falls in the Elderly (SAFE) Laboratory at the General Clinical Research Center (GCRC) at the Beth Israel Deaconess Medical Center (BIDMC). The experimental study includes additional measurements, but for the analysis in this manuscript we received data stripped of all identifiers. A similar protocol was used in previous studies, see e.g., Novak et al. (2007).

Parameter Identification

Physiological quantities vary significantly between individuals, and as discussed above, nominal parameter values do not accurately describe dynamics observed within one

Table 4 Initial and optimized parameter values for the 11 compartment model. Columns two and six are nominal parameter values. Columns three and seven give the optimized parameter values when all 52 parameters were optimized. Columns four and eight give the optimized parameter values when the top 22 sensitive parameters were optimized and the insensitive parameters remained fixed at their nominal values

Parameter	Initial	Optimized, 52	Optimized, 22	Parameter	Initial	Optimized, 52	Optimized, 22
R_{av}	0.006	0.004	–	v_{lv}	9.900	9.425	9.010
R_{au}	0.048	0.104	–	θ_{lv}	0.951	0.871	1.323
R_{aup}	1.284	1.354	1.104	$t_{diff,lv}$	0.094	0.107	–
R_{al}	0.321	0.449	–	$t_{min,lv}$	0.186	0.177	0.101
R_{alp}	9.629	9.967	9.601	$p_{min,lv}$	0.842	0.563	0.659
R_{vl}	0.321	0.346	–	$p_{diff,lv}$	0.316	0.423	–
R_{vu}	0.032	0.014	–	η_{lv}	17.500	18.326	20.528
R_{mv}	0.014	0.015	–	ϕ_{lv}	1.000	1.065	1.511
R_{vc}	0.385	0.623	–	a_a	0.0030e − 2	0.001e − 2	–
R_{acp}	3.852	3.832	3.688	c_a	6.400	6.630	4.765
R_{ac}	0.193	0.115	–	b_a	5.000	4.183	–
R_v	0.013	0.006	–	d_a	1.000	1.340	–
C_a	0.445	0.465	–	n_a	2.000	2.369	2.669
C_{au}	1.649	1.870	1.958	m_a	2.200	1.977	–
C_{al}	0.200	0.300	–	v_a	9.900	10.157	–
C_{ac}	0.354	0.180	0.079	θ_a	0.951	0.886	0.910
C_{vl}	3.335	3.357	1.463	$t_{diff,la}$	0.094	0.168	–
C_{vu}	26.153	27.370	48.540	$t_{min,la}$	0.186	0.138	–
C_v	11.982	13.099	–	$p_{min,la}$	0.842	1.055	0.600
C_{vc}	8.040	8.585	–	$p_{diff,la}$	0.316	0.427	–
a_{lv}	0.0003	0.0004	–	η_a	17.500	17.627	–
c_{lv}	6.400	6.657	4.896	ϕ_a	1.000	1.303	0.666
b_{lv}	5.000	4.075	–	A_{acp}	0.300	0.289	–
d_{lv}	1.000	0.997	–	C_{af}	0.115	0.094	–
n_{lv}	2.000	2.716	3.421	R_{af}	0.032	0.074	–
m_{lv}	2.200	1.954	1.378	R_{afp}	11.042	11.572	7.105

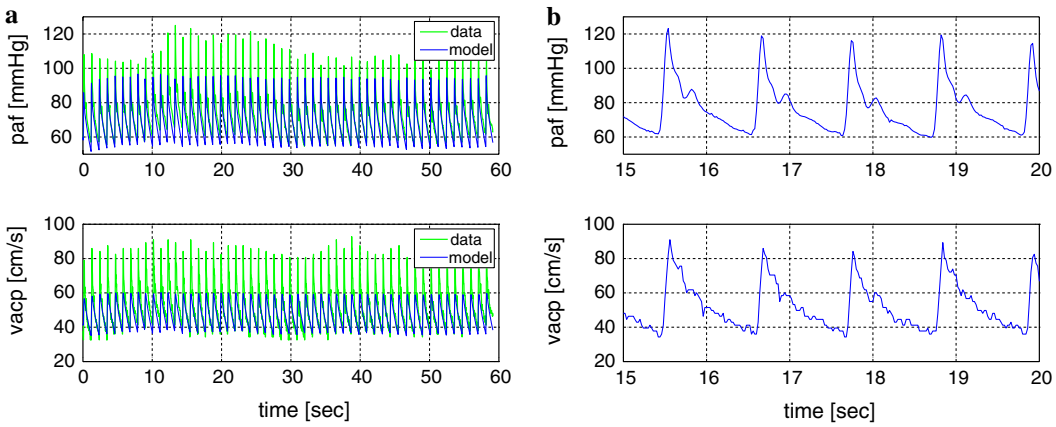

Fig. 2 Data for finger blood pressure $p_{af}(t)$ (mmHg) (top panel) and cerebral blood flow velocity $v_{acp}(t)$ (cm/s) (bottom panel). Data (gray line) are shown in (**a**) for $0 < t < 60$ s, which represent the time interval in which the subject is sitting down with his/her legs elevated at 90 degrees, and $15 < t < 20$ s in (**b**) to show a zoomed in picture of the waveform. Data was measured at 50 Hz. The black line in (**a**), shows simulations with nominal parameter values

subject. To identify model parameters that characterize a given time-series dataset we used a weighted least-squares formulation minimizing the errors between the blood pressure and blood flow velocity data and the model outputs. This weighted least-squares cost functional is given by

$$\begin{aligned}\hat{J} = &\frac{1}{N\bar{p}^d_{af}}\sum_{i=1}^{N}\left|p^d_{af}(t_i)-p^c_{af}(t_i)\right|^2\\ &+\frac{1}{N\bar{v}^d_{\mathrm{acp}}}\sum_{i=1}^{N}\left|v^d_{\mathrm{acp}}(t_i)-v^c_{\mathrm{acp}}(t_i)\right|^2\\ &+\frac{1}{M\bar{p}^d_{af,\mathrm{sys}}}\sum_{i=1}^{M}\left|p^d_{af,\mathrm{sys}}(t_i)-p^c_{af,\mathrm{sys}}(t_i)\right|^2\\ &+\frac{1}{M\bar{p}^d_{af,\mathrm{dia}}}\sum_{i=1}^{M}\left|p^d_{af,\mathrm{dia}}(t_i)-p^c_{af,\mathrm{dia}}(t_i)\right|^2\\ &+\frac{1}{M\bar{v}^d_{\mathrm{acp,sys}}}\sum_{i=1}^{M}\left|v^d_{\mathrm{acp,sys}}(t_i)-v^c_{\mathrm{acp,sys}}(t_i)\right|^2\\ &+\frac{1}{M\bar{v}^d_{\mathrm{acp,dia}}}\sum_{i=1}^{M}\left|v^d_{\mathrm{acp,dia}}(t_i)-v^c_{\mathrm{acp,dia}}(t_i)\right|^2,\end{aligned}$$

where p_{af} is blood pressure in the finger and $v_{\mathrm{acp}} = q_{\mathrm{acp}}/A_{\mathrm{acp}}$ is cerebral blood flow velocity, and A_{acp} represents the cross-sectional area of the middle cerebral artery. The subscripts c and d denote computed versus experimental values, and N is the number of data points in the time-series. Each term in the functional is weighted by the average of the data used in that term, denoted by $\bar{p}$ and $\bar{v}$. To get correct representation of the pulse amplitude, special emphasis was placed on capturing both peaks and valleys of the waveform. This is done by including terms minimizing the difference between systolic and diastolic values. The time series to be analyzed contains M periods, thus there will be M systolic and diastolic values.

Since data are only available for two locations, the above least squares cost functional is not able to ensure correct physiological ranges for internal states. In particular, we observed that the model overestimated the baseline aortic valve resistance defined in (6), which gave rise to an unphysiologically large discrepancy between the left ventricular $p_{\mathrm{lv,sys}}$ systolic pressure and the systolic aortic pressure $p_{\mathrm{a,sys}}$, Boron and Boulpaep (2003). To avoid the large pressure discrepancy, we added a constraint minimizing the error between the systolic ventricular pressure and the systolic aortic pressure. Thus an effective cost functional can be written as

$$J = \hat{J} + \frac{1}{M\bar{p}^d_{\mathrm{a,sys}}}\sum_{i=1}^{M}\left|p^c_{\mathrm{a,sys}}(t_i)-p^c_{\mathrm{lv,sys}}(t_i)\right|^2. \tag{8}$$

To identify parameters that minimize the effective cost functional J we used the Nelder–Mead algorithm Kelley (1999), which is based on cost functional evaluations on sequences of simplexes. Optimizations were run using Matlab 6.5 on a 14-node cluster at Roskilde University, Denmark, each node with an Intel Pentium 4 2.26 GHz processor with 1GB RAM. Identification of all 52 parameters took 37 h. Simulation results with the model using the optimized parameters are shown in Fig. 3a and optimized parameters are listed in Table 4.

Sensitivity Analysis

Results discussed above shows that it is possible to identify 52 parameters. However, due to the large number of parameters the solution to this optimization problem is not unique, i.e., a small variation of the nominal parameter values can lead to large changes in estimates for optimized parameter values, in particular for parameters that are insensitive. Thus, to better understand the dependence of the data on the model parameters, we have analyzed the sensitivity of the model state variables that represent the data to each of the parameters. We anticipate that this will result in a subset of identifiable parameters that when optimized is able to predict pressure and velocity dynamics observed in the data.

To derive sensitivity equations for our system of equations described in (7), we use the basic differential equation analysis approach described by Eslami (1994) and Frank (1978). Following this approach we define the relative sensitivity S_{ij} of the state X_i to parameter μ_j non-dimensionalized by the state X_i and the parameter value μ_j as

$$S_{ij}(t,\mu)\big|_{\mu=\mu_0} = \frac{\partial X_i(t,\mu)}{\partial \mu_j}\frac{\mu_j}{X_i(t,\mu)}\bigg|_{\mu=\mu_0}, \quad \mu_j, X_i(t,\mu) \neq 0. \tag{9}$$

Here $\mu_0 = [\mu_{1,0} \ldots \mu_{52,0}]$ denote the nominal values for the parameters, and we assume all state variables are continuous. As shown in Fig. 4, $S_{ij}(t,\mu)$ is a function of time.

Our goal is to separate model parameters into two groups, sensitive and insensitive. Therefore, we computed a maximum relative sensitivity $\mathbf{S_j}$ composite over all states and times for each parameter of the form

$$\begin{aligned}\mathbf{S_j} &= \max_i\left(\max_k S_{ij}(t,\mu)\right)\Big|_{\mu=\mu_0}\\ &= \max_i\left(\max_k \frac{dX_i(t_k,\mu)}{d\mu_j}\frac{\mu_j}{X_i(t_k,\mu)}\right)\Big|_{\mu=\mu_0}.\end{aligned} \tag{10}$$

Because data is only available for the two quantities, finger pressure p_{af} and cerebral blood flow velocity $v_{\mathrm{acp}} = q_{\mathrm{acp}}/A_{\mathrm{acp}}$, where $q_{\mathrm{acp}} = (p_{\mathrm{ac}} - p_{\mathrm{vc}})/R_{\mathrm{acp}}$, the maximum is computed over these three states $i = p_{\mathrm{af}}$, p_{ac}, and p_{vc}.

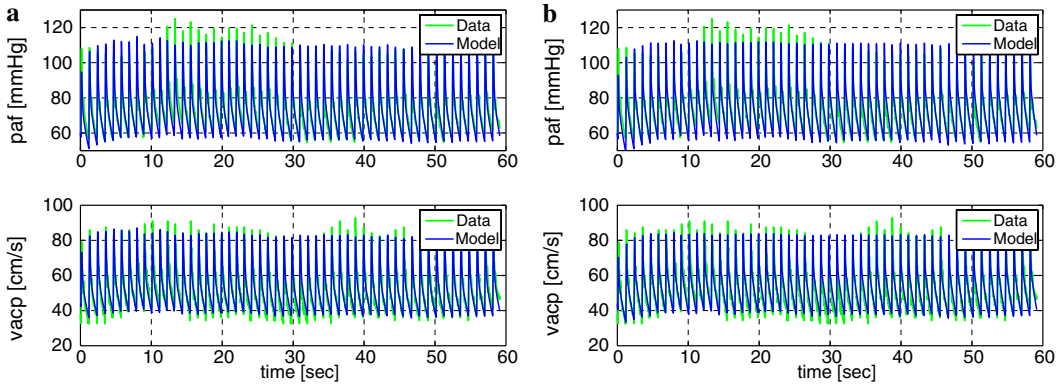

Fig. 3 Each panel shows finger pressure p_{af} (top) and cerebral blood flow velocity v_{acp} (bottom) data and model solutions. (**a**) Model with 52 parameters optimized, cost of 1.77. (**b**) Model with the 22 most sensitive parameters optimized, cost of 1.93

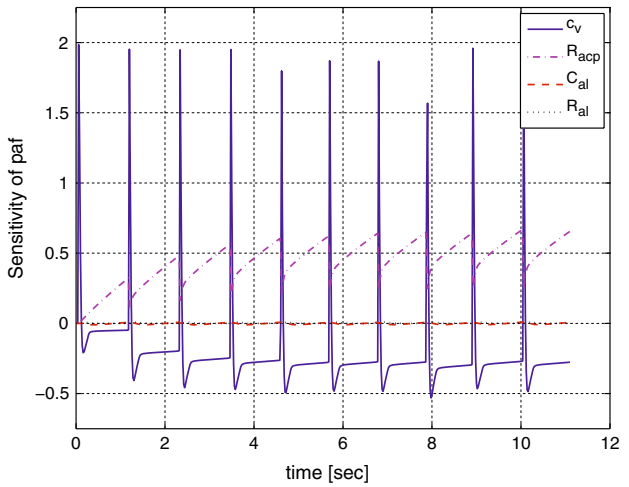

Fig. 4 Plots of the relative sensitivity $S_{p_{af},j}$, where j is parameters c_v, R_{acp}. C_{al}, and R_{al}

To compute the partial derivatives $\partial X_i/\partial \mu_j$, also referred to as quasi-state variables, each differential equation of the form (7) is differentiated with respect to each parameter, assuming that the partial derivatives commute

$$\frac{\partial}{\partial \mu_j}\frac{dX_i}{dt} = \frac{d}{dt}\frac{\partial X_i}{\partial \mu_j} = \frac{\partial}{\partial \mu_j}F_i(X,\mu). \tag{11}$$

The sensitivities in (11) are to be solved simultaneously with the state equations in (7). Together these two systems of equations result in $11 + 11 \times 52 = 583$ equations for the states $\{p_i,V_i\}$ augmented with the quasi-state solutions $\partial X_i/\partial \mu_j$. Thus the full solution is the 11 states and 572 quasi-states.

To get a better understanding for the form of the sensitivity equations, we have derived the equation predicting the sensitivity $S_{p_{af},R_{al}}$, which can be computed by differentiating (2) with respect to R_{al},

$$\frac{d}{dt}\left(\frac{\partial p_{af}}{\partial R_{al}}\right) = \frac{1}{C_{af}}\left[\frac{1}{R_{af}}\left(\frac{\partial p_a}{\partial R_{al}} - \frac{\partial p_{af}}{\partial R_{al}}\right) - \frac{1}{R_{afp}}\left(\frac{\partial p_{af}}{\partial R_{al}} - \frac{\partial p_v}{\partial R_{al}}\right)\right],$$

solving for $\partial p_{af}/\partial R_{al}$, and multiplying by $R_{al}/p_{af}(t)$. The resulting solution is shown in Fig. 4, and together with Table 5 we see that max sensitivity of p_{af} with respect to R_{al} is 0.0008. In other words, this parameter is very insensitive (compare graphs on Fig. 4). The remaining 571 equations can be derived using similar considerations. However, deriving sensitivity equations using the analytical approach exemplified above is tedious and error prone. Alternatively, sensitivities can be derived using a computational approach, either using finite differences, which may cause difficulties in multi-scale problems, or using automatic differentiation (AD), which uses the chain rule to evaluate derivatives to machine precision. The latter approach was used to derive sensitivities for the cardiovascular model. To apply automatic differentiation, we exploit the chain rule to rewrite (11) as

$$\begin{aligned}\frac{\partial}{\partial \mu_j}\frac{dX_i}{dt} &= \frac{\partial}{\partial \mu_j}F_i(X_1,\ldots,X_{11},\mu_1,\ldots,\mu_{52}) \\ &= \sum_{k=1}^{11}\left(\frac{\partial F_i}{\partial X_k}\frac{\partial X_k}{\partial \mu_j}\right) + \frac{\partial F_i}{\partial \mu_j},\end{aligned} \tag{12}$$

where the Jacobians $\partial F/\partial X$ and $\partial F/\partial \mu$ are calculated using AD, and $\partial X/\partial \mu$ are the quasi-state variables. Thus, the right hand side of the system of ODE's in (11) is constructed with the components of the Jacobians and the quasi-state variables. Solutions to quasi-state equations give time-series for $dX_i/d\mu_j(t_k)$, where $k = 1 \ldots N$, i represents the state variables, and j represents each of the 52 parameters.

The above derivation of sensitivity equations required that the derivatives of the states with respect to each of the parameters are differentiable. The system of equations analyzed in this study includes two groups of equations that

Table 5 Ranked (most-to-least) sensitivities for 11 compartment model for the pressures p_f, p_{ac} and p_{vc} with respect to all parameters

Rank	Parameter	p_{af}	p_{ac}	p_{vc}	Sensitivity	Rank	Parameter	p_{af}	p_{ac}	p_{vc}	Sensitivity
1	c_{lv}	**2.029**	0.798	0.054	2.029	27	v_{la}	**0.139**	0.122	0.013	0.139
2	n_{lv}	**1.981**	1.377	0.043	1.981	28	C_a	**0.135**	0.076	0.007	0.135
3	θ_{lv}	**1.270**	0.432	0.070	1.270	29	$t_{diff,lv}$	**0.133**	0.039	0.007	0.133
4	R_{aup}	**1.084**	1.052	0.189	1.084	30	C_v	**0.122**	0.115	0.074	0.122
5	R_{alp}	0.401	0.390	**0.944**	0.944	31	m_{la}	**0.092**	0.058	0.052	0.092
6	ϕ_{lv}	**0.876**	0.357	0.022	0.876	32	η_{la}	**0.086**	0.080	0.008	0.086
7	C_{vu}	**0.874**	0.862	0.823	0.874	33	R_{vc}	**0.074**	0.065	0.058	0.074
8	R_{acp}	0.679	**0.797**	0.166	0.797	34	R_{au}	**0.067**	0.048	0.003	0.067
9	n_{la}	**0.788**	0.743	0.122	0.788	35	b_{lv}	**0.056**	0.054	0.005	0.056
10	$p_{min,lv}$	**0.725**	0.279	0.019	0.725	36	C_{af}	**0.051**	0.010	0.001	0.051
11	c_{la}	**0.668**	0.625	0.066	0.668	37	$t_{diff,la}$	**0.050**	0.045	0.005	0.050
12	θ_{la}	**0.553**	0.518	0.049	0.553	38	$p_{diff,lv}$	**0.049**	0.021	0.001	0.049
13	$t_{min,lv}$	**0.476**	0.157	0.026	0.476	39	R_{vu}	**0.042**	0.030	0.036	0.042
14	C_{vl}	0.031	0.030	**0.416**	0.416	40	b_{la}	0.010	0.008	**0.022**	0.022
15	R_{afp}	**0.382**	0.354	0.005	0.382	41	R_{af}	**0.022**	0.001	0.000	0.022
16	v_{lv}	**0.378**	0.110	0.018	0.378	42	R_{mv}	**0.021**	0.020	0.001	0.021
17	ϕ_{la}	**0.354**	0.296	0.027	0.354	43	$p_{diff,la}$	**0.020**	0.015	0.001	0.020
18	C_{au}	**0.323**	0.284	0.048	0.323	44	R_v	**0.019**	0.017	0.015	0.019
19	m_{lv}	**0.288**	0.184	0.033	0.288	45	C_{al}	**0.010**	0.009	0.003	0.010
20	η_{lv}	**0.246**	0.092	0.007	0.246	46	R_{av}	**0.008**	0.003	0.000	0.008
21	$p_{min,la}$	**0.236**	0.220	0.023	0.236	47	R_{al}	**0.008**	0.007	0.007	0.008
22	C_{ac}	0.035	**0.205**	0.005	0.205	48	a_{lv}	**0.003**	0.003	0.000	0.003
23	$t_{min,la}$	**0.199**	0.185	0.020	0.199	49	d_{lv}	**0.002**	0.001	0.000	0.002
24	R_{vl}	0.010	0.009	**0.173**	0.173	50	a_{la}	0.001	0.001	**0.002**	0.002
25	R_{ac}	0.032	**0.163**	0.003	0.163	51	d_{la}	**0.001**	0.000	0.000	0.001
26	C_{vc}	**0.143**	0.142	0.110	0.143	52	A_{acp}	0	0	0	0

Values in boldface are the maximum values for each parameter

do not immediately appear to be fully differentiable: the three valves in (e.g., (6)) and the heart functions (e.g., (4), (5)). The valve equations, while piecewise continuous, do not have derivatives at the cusps between the exponential function and the constant. To construct a smooth function that is differentiable, we adapted a smooth approximation, Chen et al. (2004), of the form

$$\min_{\epsilon}(x_1, x_2) = -\epsilon \ln\left(\sum_{i=1}^{2} e^{-x_i/\epsilon}\right),$$

using an ϵ of 0.1. In the heart function, the partial derivative of the ventricle activation function f_i defined in (5) with respect to the parameter n is given by

$$\frac{\partial f}{\partial n} = \tilde{p} n^{-n} m^{-m} \left(\frac{\beta(n)}{n+m}\right)^{(-n-m)} \tilde{t}^n (\beta(n) - \tilde{t})^m \left(\ln(\tilde{t}) - \ln(m) - \ln\left(\frac{\beta(n)}{n+m}\right)\right) \left[t_{pv} \frac{-m}{n^2}\right],$$

which is undefined at $\tilde{t} = 0$. However, using L'Hospital's Rule, it is possible to determine the limit of this portion of the equation as $\tilde{t} \to 0$. To calculate this limit we let

$$K_n = \tilde{p} n^{-n} m^{-m} \left(\frac{\beta(n)}{n+m}\right)^{(-n-m)} \left[t_{pv} \frac{-m}{n^2}\right],$$

yielding

$$\lim_{\tilde{t}\to 0} K_n \tilde{t}^n (\beta - \tilde{t})^m \ln(\tilde{t}) = \lim_{\tilde{t}\to 0} K_n \frac{1/\tilde{t}}{-n\tilde{t}^{-n-1} m (\beta - \tilde{t})^{-m-1}} = 0.$$

Since $f = 0$ at $\beta < \tilde{t} < T$, $\partial f_i / \partial n = 0$. Thus we have continuity of $\partial f / \partial n$ if we assign $\partial f / \partial n = 0$ at $t = 0$, because $\tilde{t} = T$ of period i while $\tilde{t} = 0$ of period $i + 1$. A similar analysis is done for the remaining partial derivatives with respect to other parameters in the heart activation function.

Results

Parameter Sensitivity

To rank parameters from the most to the least sensitive, we solved equations (1) predicting pressures in each of

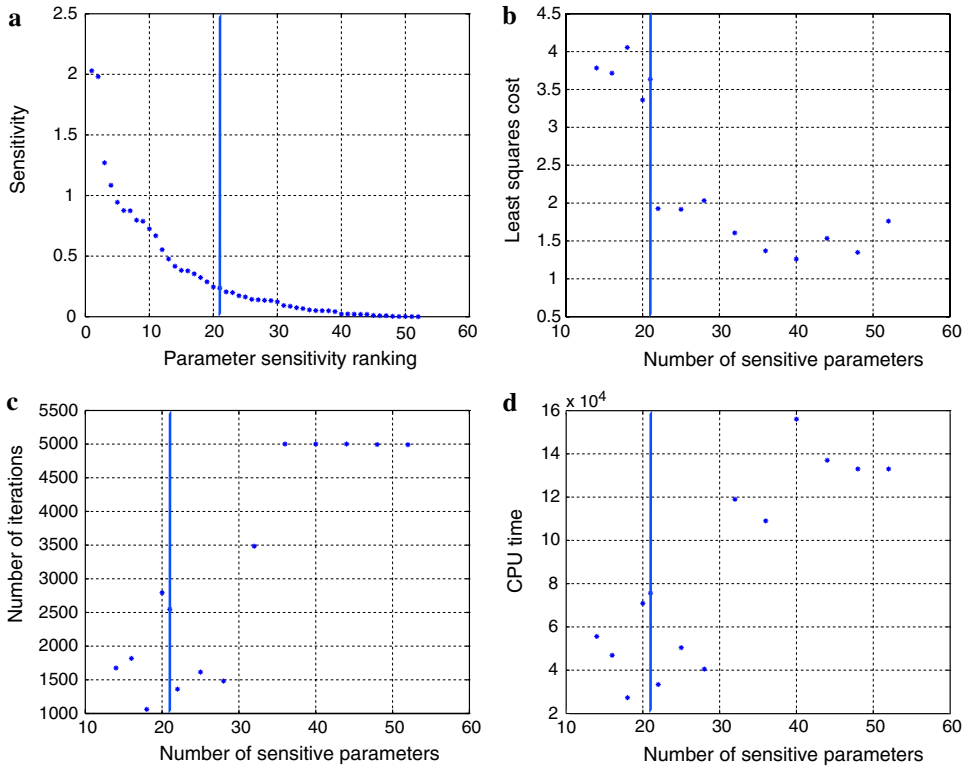

Fig. 5 (**a**) Sensitivities of each parameter versus their relative ranking. (**a–d**) Results of parameterizing the system by optimizing a decreasing number of sensitive parameters while keeping an increasing number of insensitive parameters fixed at their nominal values. (**b**, **c**, **d**) depict the least squares cost, the number of iterations, and the computational time versus the number of sensitive parameters identified, respectively. The vertical lines are each at 21, the number of sensitive parameters

the arterial and venous compartments and (3) predicting volumes of the atrium and the ventricle, coupled with the system of sensitivity equations as written in (12). Then, we calculated the max sensitivity for each parameter as described in (10). Results of these calculations gave rise to the ranking shown in Fig. 5a and Table 5. Results depicted on this graph suggests a decreasing exponential relationship between sensitivity $\mathbf{S_j}$ and the relative ranking. Figure 5b–d show the results of optimizations run with a systematic reduction in the number of parameters optimized. The weighted least squares cost, the number of optimization iterations, and computational time were recorded. Figure 5b indicates a negligible change in cost from 1.77 as the number of "estimated" parameters are reduced from 52. Identification of the 22 most sensitive parameters gives a cost increase of roughly 8% to 1.93, yet optimizing 21 parameters increases the cost by more than 100% to 3.63. Hence, we name the top 22 parameters "sensitive", and maintain that acceptable model fit can be attained by only optimizing these 22, with a resultant reduction in the number of iterations needed to half of the starting number. Figure 3 compares results for finger blood pressure and cerebral blood flow velocity obtained when all 52 model parameters are identified (left panel), with a cost of 1.77, and when only the top 22 parameters are identified (right panel), with a cost of 1.93. Table 4 shows optimized parameters. Analysis of these two graphs reveal only slight qualitative differences between the results.

Finally, it should be noted that A_{acp} does not appear in the state equations. Therefore its sensitivity is not calculated as in the above equations and as a result it is ranked at the bottom of the sensitivity list with a sensitivity equal to zero. Optimizations run for a fixed nominal value of A_{acp} show a negligible change in cost compared to optimizations that identified A_{acp}. These results confirm our hypothesis that the parameter A_{acp} is not sensitive.

Model Reduction

Sensitivity ranking of parameters shown in Table 5 can also be used to reduce the complexity of the model. In general, to reduce the model, compartments comprised of sensitive parameters are retained while those mainly consisting of insensitive parameters may be eliminated. However, before a compartment is eliminated several factors must be taken into account. The system must have a heart acting as a pump to raise the pressure against its gradient, so one or both heart compartments are retained. Second, separation between the brain and the rest of the body must be maintained because data used for model validation are collected both in the brain (cerebral blood flow velocity) and in the body (finger blood pressure). Finally, the various model components are related, thus if one compartment is removed, it may impact dynamics of other elements, which may impact the solution. Furthermore,

if the data used for model comparison are not adequate, it will not be possible to accurately predict the distribution of blood between compartments. However, instead of removing a compartment to remove a parameter, it may be possible to keep one parameter constant, while other parameters are identified by minimizing the weighted least squares error between the data and the model.

We first observe that each atrial parameter is significantly less sensitive than its corresponding ventricle parameter. This makes sense physiologically since the atrium acts primarily as a reservoir and to a lesser extent as a small priming pump, leaving the primary driver of the pressure gradient to the ventricle. Therefore the atrium is removed from the model. We next consider the portion of the system below the level of the heart. Peripheral resistances R_{alp}, R_{aup}, and R_{afp} are all sensitive, as well as compliances C_{vl}, C_{vu}, and C_{au}. Instead of concluding immediately that this entire portion of the circulation is sensitive and therefore necessary to the model, we consider these results in light of the physiology and the data. Since we only have data for the brain and the arteries near the heart, model results obtained for the remainder of the body are dependent upon each other. In other words, many combinations of pressures, resistances, and compliances could comprise the same total resistance and flow in the body below the heart, leading to the same solution for arterial blood pressure and cerebral blood flow velocity. The differentiation between the upper and lower bodies that was necessary for modeling a data set with standing, i.e., gravitational effects, is not necessary with our steady-state sitting data. Therefore we conclude that sensitive parameters are such because they are dependent upon each other to provide an effect equal to what would occur with a combined upper and lower body. In addition, note that finger parameters C_{af} and R_{af} are ranked insensitive, at 36 and 41, respectively. This is likely because the proportion of blood flowing to the arm is small compared to the rest of the body and therefore not significant to the model parameterization.

In summary, we eliminated compartments representing the finger and the left atrium and combined the upper and lower body compartments. The resulting compartment model has seven compartments representing the left ventricle, aorta and vena cava, arteries and veins in the body as well as in the brain, see Fig. 6. Elimination of the atrium reduces the number of parameters by 15 (including R_v); at the same time, elimination of the arterial and venous compartments reduces the number of parameters by eight, hence, the proposed reduced model has seven differential equations and 29 parameters, compared with 11 differential equations and 52 parameters for the full model. Compared against the full model of with 52 parameters, which had a cost of 1.77, the reduced model cost is 1.58. Qualitatively the model solution fits the data similarly in both cases. Equations for this model can be found in the Appendix.

As we did with the full model, we carried out sensitivity analysis to rank the parameters with respect to pressures that represent the data to be studied. For this model these pressures are: p_a, p_{ac}, and p_{vc}. Similar to the full model, the heart parameters are shown to be the most sensitive (n, c, θ, ϕ, t_{min}, and p_{min}) though they appear in a slightly different order. The most sensitive non-heart parameter for this model is R_{asp}. This compares well with the full model where R_{aup} and R_{alp} showed high sensitivity. Also both the full model and the reduced model shows high sensitivity to R_{acp} (ranked 9 and 5 in each, respectively) because it is explicitly part of one of the equations that directly represents the data. Finally, it was found from analyses similar to those done with full model that 20 sensitive parameters can be accurately estimated in the small model.

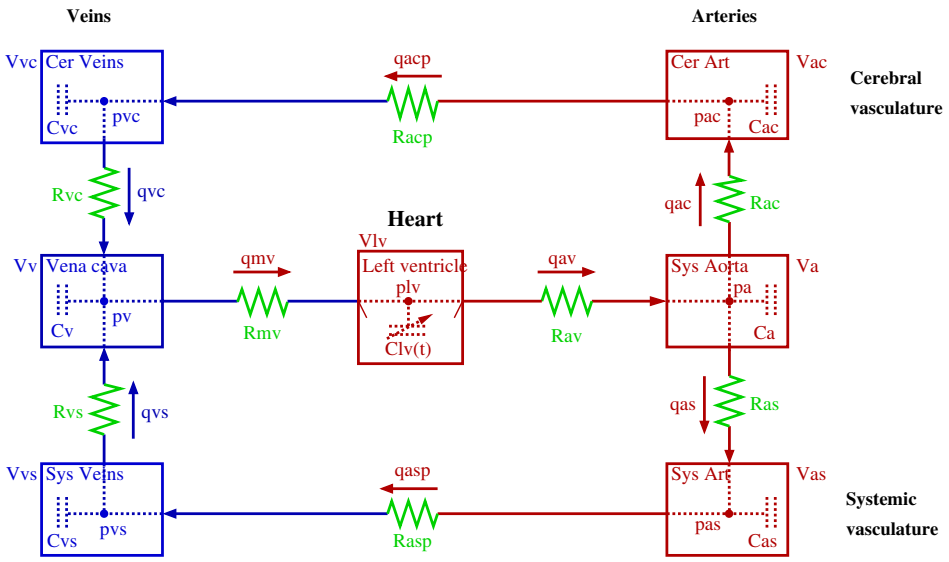

Fig. 6 The 7-compartment model of systemic circulation, including arteries (a) and veins (v) in the brain (cerebral vasculature, c), the body (systemic vasculature, s), and the left ventricle (lv)

Discussion

In this study we have shown that it is possible to accurately predict 22 of 52 parameters for a single dataset in our compartment model of systemic blood pressure and blood flow, while retaining model fit to data as seen in Fig. 3. Sensitive parameters have physiological significance, most of which characterize the left ventricle waveform or represent lumped peripheral resistances. Hence, to identify parameter values for multiple datasets only the most sensitive parameters need to be identified for each of the datasets, and it would be reasonable to use literature estimates for the least sensitive parameters and keep these fixed at nominal values. Based on these predictions, it would then be possible to calculate means and standard deviations for each parameter for a given group of subjects and compare values between different groups of subjects. We have also shown that it is possible to use sensitivity information to reduce the proposed model and design a simpler model that has a similar number of sensitive parameters. We do not however make any conclusions on sensitivities during postural change from sitting to standing. We hypothesize in that case that differentiation between upper and lower body due to gravitational effects would be necessary. Further investigations include performing the sensitivity analysis on the previously developed postural change model, Olufsen et al. (2005).

Looking specifically at the top 22 parameters of the original model, it is seen in Table 6 that the majority of the top sensitive parameters characterize the heart functions, particularly the ventricle. These parameters are largely responsible for describing the timing and magnitude of peak ventricular heart pressure p_{pv} and t_{pv}, respectively. Because the heart function drives the model, and the peak pressure and waveform timing in the heart are similar to that in the aorta and nearby arteries, Boron and Boulpaep (2003), it is consistent that the model fit would be most sensitive to these parameters. Not much is known about these parameters a priori, as opposed to those that are estimated from known physiological quantities, so finding parameter values for an individual patient is key for model parameterization. The peripheral resistances R_{aup}, R_{alp}, R_{acp}, and R_{afp} characterize the largest pressure drops, so it makes sense that they have a large impact on the solution.

Conversely, we correlate insensitivity of parameters with known physiology. Each atrial parameter is less sensitive than its corresponding ventricular parameters. This is consistent with the fact that maximum atrial pressure is approximately an order of magnitude less than maximum

Table 6 Top 22 sensitive parameters and their effect on the model

Parameter	Role in model	Effect on model with increase in parameter value
c_{lv}	Ventricular contractility	Increase developed and systolic pressure
n_{lv}	Exponent in ventricle polynomial	Ventricular peak pressure moves right in time
θ_{lv}	Median of ventricular t_p sigmoid	Increase median time for peak pressure at given heart rate
R_{aup}	Resistance, upper body arterioles	Increase upper body pressure drop
R_{alp}	Resistance, lower body arterioles	Increase lower body pressure drop
ϕ_{lv}	Median of ventricular p_p sigmoid	Increase median peak pressure at given heart rate
C_{vu}	Compliance, upper body veins	Increase p_{af} and v_{acp}
R_{acp}	Resistance, cerebral arterioles	Increase cerebral pressure drop
n_{la}	Exponent in atrium polynomial	Atrial peak pressure moves right in time
$p_{\text{min,lv}}$	Minimum of ventricular p_p sigmoid	Increase minimum possible peak pressure at given heart rate
c_{la}	Atrial contractility	Increase developed and systolic pressure
θ_{la}	Median of atrial t_p sigmoid	Increase median time for peak pressure at given heart rate
$t_{\text{min,lv}}$	Minimum of t_p sigmoid	Increase minimum possible peak pressure at given heart rate
C_{vl}	Compliance, lower body veins	Increase p_{af} and v_{acp}
R_{afp}	Resistance, finger arterioles	Increase finger pressure drop
v_{lv}	Steepness of ventricular t_p sigmoid	Increase distance from median time at given heart rate
ϕ_{la}	Median of atrial p_p sigmoid	Increase median peak pressure at given heart rate
C_{au}	Compliance, upper body arteries	Increase p_{af} and v_{acp}, narrow waveforms
m_{lv}	Exponent in ventricle polynomial	Ventricular peak pressure moves left in time
η_{lv}	Steepness of ventricular p_p sigmoid	Increase distance from median time at given heart rate
$p_{\text{min,la}}$	Minimum of atrial p_p sigmoid	Increase minimum possible peak pressure at given heart rate
C_{ac}	Compliance, cerebral arteries	Narrow v_{acp} waveform

ventricular pressure, Boron and Boulpaep (2003), and the atrium primarily acts as a primer pump. As another example, the position of d_{lv} representing the volume-independent component of developed pressure for the ventricle, is at the bottom of the sensitivity ranking. Physiologically this could mean several things such as: d_{lv} could be virtually identical between young adult subjects; it could be scaled based on the subject but its exact value is not critical for model fit; or that its place in the model is not necessary. In immediate future investigations we would choose to fix parameters such as these at their estimated from literature values as stated previously and assume that such values are accurate enough for model fit.

To reach the results in this study we used automatic differentiation to calculate the gradients used to find the sensitivities of each parameter with respect to each of the state variables. While automatic differentiation algorithms are well-developed and have long been used in languages such as Fortran, Matlab algorithms are fairly new, Coleman and Verma (1998) and Forth and Ketzscher (2004). The main disadvantage of the Matlab algorithms is that they are slow relative to Fortran and C++. One numerical solve of the model including sensitivity equations takes about 30 min, and an optimization run with the Nelder–Mead simplex method not including the sensitivity equations takes a day and a half. As we wish to analyze multiple subjects' data and expand to different populations, speed will become a necessity. Combining the 30-min-per-iteration automatic differentiation with a many-iteration optimization routine in Matlab is not reasonable for this purpose. Therefore we intend to explore automatic differentiation algorithms in Fortran and C++. In addition, using automatic differentiation for this problem makes it feasible to investigate the use of gradient-based optimization methods Kelley (1999), which may lead to more efficient parameter identification.

Finally, our sensitivity analysis does not tell us anything about the correlation between parameters. The body is a closed system of interacting parts, a model of which would likely contain parameters that act dependently on each other. Generalized sensitivities, discussed by Thomaseth and Cobelli (1999), may elucidate interactions between parameters and also reveal time intervals for which a parameter is most sensitive. In future work we plan to investigate the use of this and other sensitivity analysis methods such as Green's method, Hwang et al. (1978).

Acknowledgments The authors wish to thank the American Institute of Mathematics for supporting this work. Authors would like to acknowledge Dr. Fink, Department of Mathematics, University of Oxford, UK, who developed the Matlab code for automatic differentiation. The work by M. S. Olufsen and H. T. Tran was supported in part by NSF-DMS Grant # 0616597. H. T. Tran was supported by NIH under Grant 9 R01 AI071915-05. C. Zapata was supported in part by NSA under Grant H98230-06-1-0098 and NSF under Grant DMS-0552571 as part of the REU summer program. V. Novak, director of the SAFE Laboratory at BIMDC was supported by NIH-NIA Harvard Older American Independence Center 2P60 AG08812-11A1, Core B.

Appendix

Equations, Full Model

(1) *Compartment ODE's:*

$$\frac{dp_a}{dt} = \left(\frac{p_{lv}(t) - p_a(t)}{R_{av}} - \frac{p_a(t) - p_{au}(t)}{R_{au}} - \frac{p_a(t) - p_{ac}(t)}{R_{ac}} - \frac{p_a(t) - p_{af}(t)}{R_{af}} \right) / C_a$$

$$\frac{dp_{au}}{dt} = \left(\frac{p_a(t) - p_{au}(t)}{R_{au}} - \frac{p_{au}(t) - p_{al}(t)}{R_{al}} - \frac{p_{au}(t) - p_{vu}(t)}{R_{aup}} \right) / C_{au}$$

$$\frac{dp_{al}}{dt} = \left(\frac{p_{au}(t) - p_{al}(t)}{R_{al}} - \frac{p_{al}(t) - p_{vl}(t)}{R_{alp}} \right) / C_{al}$$

$$\frac{dp_{af}}{dt} = \left(\frac{p_a(t) - p_{af}(t)}{R_{af}} - \frac{p_{af}(t) - p_v(t)}{R_{afp}} \right) / C_{af}$$

$$\frac{dp_{ac}}{dt} = \left(\frac{p_a(t) - p_{ac}(t)}{R_{ac}} - \frac{p_{ac}(t) - p_{vc}(t)}{R_{acp}} \right) / C_{ac}$$

$$\frac{dp_v}{dt} = \left(\frac{p_{vu}(t) - p_v(t)}{R_{vu}} + \frac{p_{vc}(t) - p_v(t)}{R_{vc}} + \frac{p_{af}(t) - p_v(t)}{R_{afp}} - \frac{p_v(t) - p_{la}(t)}{R_v} \right) / C_v$$

$$\frac{dp_{vu}}{dt} = \left(\frac{p_{vl}(t) - p_{vu}(t)}{R_{vl}} + \frac{p_{au}(t) - p_{vu}(t)}{R_{aup}} - \frac{p_{vu}(t) - p_v(t)}{R_{vu}} \right) / C_{vu}$$

$$\frac{dp_{vl}}{dt} = \left(\frac{p_{al}(t) - p_{vl}(t)}{R_{alp}} - \frac{p_{vl}(t) - p_{vu}(t)}{R_{vl}} \right) / C_{vl}$$

$$\frac{dp_{vc}}{dt} = \left(\frac{p_{ac}(t) - p_{vc}(t)}{R_{acp}} - \frac{p_{vc}(t) - p_v(t)}{R_{vc}} \right) / C_{vc}$$

$$\frac{dV_{lv}}{dt} = \frac{p_{la}(t) - p_{lv}(t)}{R_{mv}(t)} - \frac{p_{lv}(t) - p_a(t)}{R_{av}(t)}$$

$$\frac{dV_{la}}{dt} = \frac{p_v(t) - p_{la}(t)}{R_v} - \frac{p_{la}(t) - p_{lv}(t)}{R_{mv}(t)}$$

Parameters include R_i (mmHg s/cm^3), C_i (cm^3/mmHg).

2) *Valve equations* R_{av}, R_{mv}, R_{vu}:

$$R_{av} = \min(R_{av,open} + e^{(-2(p_{lv} - p_a))}, 20)$$

$$R_{mv} = \min(R_{mv,open} + e^{(-2(p_{la} - p_{lv}))}, 20)$$

$$R_{vu} = \min(R_{vu,open} + e^{(-2(p_{vu} - p_v))}, 20)$$

3) *Left atrium and ventricle:*

$$p_j(t) = a_j(V_j(t) - b_j)^2 + (c_j V_j(t) - d_j) f_j(t),\ j = \mathrm{lv}, \mathrm{la}$$

$$f_j(t) = \begin{cases} \tilde{p}_j(H) \dfrac{\tilde{t}^{n_j} (\beta(H) - \tilde{t})_j^m}{n_j^{n_j} m_j^{m_j} [(\beta_j(H))/(m_j + n_j)]^{m_j + n_j}} & 0 \le \tilde{t} \le \beta_j(H) \\ 0 & \beta_j(H) < \tilde{t} < T \end{cases}$$

$$\tilde{t} = \mathrm{mod}(t, T)$$

$$t_j = (t_{diff,j}) \frac{\theta_j^{v_j}}{H^{v_j} + \theta_j^{v_j}} + t_{\min,j}$$

$$\tilde{p}_j = (p_{diff,j}) \frac{H^{\eta_j}}{H^{\eta_j} + \phi_j^{\eta_j}} + p_{\min,j}$$

$$\beta_j(H) = \frac{n_j + m_j}{n_j} t_j(H)$$

Equations, Reduced Model

(1) *Compartment ODE's:*

$$\frac{dp_\mathrm{a}}{dt} = \left(\frac{p_\mathrm{lv} - p_\mathrm{a}}{R_\mathrm{av}} - \frac{p_\mathrm{a} - p_\mathrm{as}}{R_\mathrm{as}} - \frac{p_\mathrm{a} - p_\mathrm{ac}}{R_\mathrm{ac}} \right) / C_\mathrm{a}$$

$$\frac{dp_\mathrm{v}}{dt} = \left(\frac{p_\mathrm{vs} - p_\mathrm{v}}{R_\mathrm{vs}} + \frac{p_\mathrm{vc} - p_\mathrm{v}}{R_\mathrm{vc}} - \frac{p_\mathrm{v} - p_\mathrm{lv}}{R_\mathrm{mv}} \right) / C_\mathrm{v}$$

$$\frac{dp_\mathrm{as}}{dt} = \left(\frac{p_\mathrm{a} - p_\mathrm{as}}{R_\mathrm{as}} - \frac{p_\mathrm{as} - p_\mathrm{vs}}{R_\mathrm{asp}} \right) / C_\mathrm{as}$$

$$\frac{dp_\mathrm{vs}}{dt} = \left(\frac{p_\mathrm{as} - p_\mathrm{vs}}{R_\mathrm{asp}} - \frac{p_\mathrm{vs} - p_\mathrm{v}}{R_\mathrm{vs}} \right) / C_\mathrm{vs}$$

$$\frac{dp_\mathrm{ac}}{dt} = \left(\frac{p_\mathrm{a} - p_\mathrm{ac}}{R_\mathrm{ac}} - \frac{p_\mathrm{ac} - p_\mathrm{vc}}{R_\mathrm{acp}} \right) / C_\mathrm{ac}$$

$$\frac{dp_\mathrm{vc}}{dt} = \left(\frac{p_\mathrm{ac} - p_\mathrm{vc}}{R_\mathrm{acp}} - \frac{p_\mathrm{vc} - p_\mathrm{v}}{R_\mathrm{vc}} \right) / C_\mathrm{vc}$$

$$\frac{dV_\mathrm{lv}}{dt} = \frac{p_\mathrm{v} - p_\mathrm{lv}}{R_\mathrm{mv}} - \frac{p_\mathrm{lv} - p_\mathrm{a}}{R_\mathrm{av}}$$

(2) *Valve equations*, R_av, *and* R_mv:

$$R_\mathrm{mv} = \min(R_\mathrm{mv,open} + e^{(-2(p_\mathrm{v} - p_\mathrm{lv}))}, 20)$$

$$R_\mathrm{av} = \min(R_\mathrm{av,open} + e^{(-2(p_\mathrm{lv} - p_\mathrm{a}))}, 20)$$

(3) *Left ventricle:* Equations for the left ventricle are identical to those displayed above.

References

Banks H, Bortz D. A parameter sensitivity methodology in the context of HIV delay equation models. J Math Biol 2005; 50(6):607–25.

Beneken J, DeWit B. A physical approach to hemodynamic aspects of the human cardiovascular system. In: Reeve E, Guyton A, editors. Physical bases of circulatory transport: regulation and exchange. Philadelphia: W.B. Saunders; 1967. p. 1–45.

Bischoff K, Brown R. Drug distribution in mammals. Chem Eng Prog Symp Ser 1966;50(66):33–45.

Boron W, Boulpaep E. Medical physiology. Philadelphia: Elsevier; 2003.

Bortz B, Nelson P. Sensitivity analysis of nonlinear lumped parameter models of hiv infection dynamics. J Math Biol 2004;66(5):1009–26.

Carmichael G, Sandu A, Potra F. Sensitivity analysis for atmospheric chemistry models via automatic differentiation. Atmos Environ 1997;31(3):475–89.

Chen X, Qi L, Teo K-L. Smooth convex approximation to the maximum eigenvalue function. J Global Opt 2004;30:253–70.

Coleman T, Verma A. ADMAT: an automatic differentiation toolbox for matlab. Technical report, Computer Science Department, Cornell University, NY; 1998.

Danielsen M, Ottesen J. Describing the pumping heart as a pressure source. J Theo Biol 2001;212:71–81.

Ebert T. Sensitivity of fitness to macro-parameter changes: an analysis of survivorship and individual growth in sea urchin life histories. Oecologia 1985;65:461–7.

Eslami M. Theory of sensitivity in dynamic systems: an introduction. Berlin: Springer-Verlag; 1994.

Forth S, Ketzscher R. High-level interfaces for the MAD (Matlab Automatic Differentiation) package. In: Neittaanmäki P, et al. editors. ECCOMAS 2004: fourth European congress on computational methods in applied sciences and engineering. European Community on Computational Methods in Applied Sciences; 2004.

Frank P. Introduction to sensitivity theory. New York: Academic Press; 1978.

Heldt T, Shim E, Kamm R, Mark R. Computational modeling of cardiovascular response to orthostatic stress. J Appl Physiol 2002; 92(3):1239–54.

Hwang J-T, Dougherty E, Rabitz S, Rabitz H. The Green's function method of sensitivity analysis in chemical kinetics. J Chem Phys 1978;69(11):5180–91.

Kappel F, Peer R. A mathematical model for fundamental regulation processes in the cardiovascular system. J Math Biol 1993;31(6):611–31.

Kelley C. Iterative methods for optimization. Philadelphia: Society for Industrial and Applied Mathematics; 1999.

Middleman S. Transport phenomena in the circulatory system. New York: Wiley-Interscience; 1972.

Nadler S, Hidalgo J, Bloch T. Prediction of blood volume in normal human adults. Surgery. 1962;51:224–32.

Novak V, Hu K, Vyas M, Lipsitz L. Cardiolocomotor coupling in young and elderly people. J Gerontol A Biol Sci Med Sci 2007; 62(1):86–92.

Olufsen M, Tran H, Ottesen J. Modeling cerebral blood flow control during posture change from sitting to standing. J Cardiovasc Eng 2004;4(1):47–58.

Olufsen M, Tran H, Ottesen J, Ellwein L, Lipsitz L, Novak V. Blood pressure and blood flow variation during postural change from sitting to standing – modeling and experimental validation. J Appl Physiol 2005;99(4):1523–37.

Olufsen M, Tran H, Ottesen J, Lipsitz L, Novak V. Modeling baroreflex regulation of heart rate during orthostatic stress. Am J Physiol 2006;291:R1355–68.

Ottesen J. Modeling of the baroreflex-feedback mechanism with time-delay. J Math Biol 1997a;36:41–63.

Ottesen J. Nonlinearity of baroreceptor nerves. Surv Math Ind 1997b;7:187–201.

Ottesen J, Danielsen M. Modeling ventricular contraction with heart rate changes. J Theo Biol 2003;222(3):337–46.

Rabitz H, Kramer M, Dacol D. Sensitivity analysis in chemical kinetics. Ann Rev Phys Chem 1983;34:419–61.

Rideout V. Mathematical and computer modeling of physiological systems. New Jersey: Prentice Hall; 1991.

Thomaseth K, Cobelli C. Generalized sensitivity functions in physiological identification. Ann Biomed Eng 1999;27:607–16.

Ursino M. Interaction between carotid baroregulation and the pulsating heart: a mathematical model. Am J Physiol 1998;44: H1733–47.